Hindawi Publishing Corporation
Mathematical Problems in Engineering
Volume 2013, Article ID 172728, 7 pages
http://dx.doi.org/10.1155/2013/172728

Research Article

Free Space Ranging Utilizing Chaotic Light

Tong Zhao,[1,2] Bing-jie Wang,[1,2] Yun-cai Wang,[1,2] and Xiao-ming Chang[1,2]

[1] *Key Laboratory of Advanced Transducers & Intelligent Control System, Ministry of Education, Shanxi, China*
[2] *Institute of Optoelectronic Engineering, College of Physics & Optoelectronics, Taiyuan University of Technology, No. 79 Yingze West Street, Taiyuan, Shanxi, China*

Correspondence should be addressed to Yun-cai Wang; wangyc@tyut.edu.cn

Received 22 October 2013; Accepted 26 November 2013

Academic Editor: Hai Yu

We report our recent works on free space ranging with chaotic light. Using a laser diode with optical feedback as chaotic source, a prototype of chaotic lidar has been developed and it can achieve a range-independent resolution of 18 cm and measurable distance of 130 m at least. And its antijamming performance is presented experimentally and numerically. Finally, we, respectively, employ the wavelet denoising method and the correlation average discrete-component elimination algorithm to detect the chaotic signal in noisy environment and suppress the side-lobe noise of the correlation trace.

1. Introduction

Light detection and ranging (lidar), as an advanced detection technology, has attracted extensive attention recently [1–3]. In the traditional lidar techniques, short-pulse or modulated continuous-wave (CW) laser is usually used as probe signal. The pulse technique, known as the time-of-flight method, achieved the measurement by detecting the power and arrival time of the reflect pulse. But there exists a drawback on the trade-off between spatial resolution and detectable distance. In comparison, the modulated CW technique uses an external modulator to modulate the phase of CW laser. Depending on the shifted phase between echo and transmit light, the target position is obtained. In this technique, the spatial resolution is determined by the bandwidth of modulated waveform. However, both of these methods cannot avoid the problem of the interference from the same systems.

To solve this problem, Takeuchi et al. [4] proposed the pseudorandom-code modulated CW lidar with unique code in each instrument. But the expensive high-speed pseudorandom-code-generator limited the development of this method. Therefore, the broad bandwidth chaotic light with characteristic of noise-like vibration and simple generated configuration had a trend of the replacement of the pseudorandom-code modulated light. Myneni et al. [5] first used the chaotic laser for ranging and then Lin and Liu [6] proposed the concept of the chaotic lidar with a proof-of-concept experiment.

Remarkably, laser diode with optical feedback is the simplest way to generate wideband chaotic signal. Based on this method, we developed a prototype of chaotic lidar and analyzed its performance. Our work mainly consists of three aspects: the introduction of the chaotic lidar [7, 8], the performance of antijamming [9], and the improvement of signal-to-noise ratio (SNR) [10]. In the following sections, they will be demonstrated, respectively.

2. Free Space Ranging Using Chaotic Light

2.1. Principle and Prototype. The experimental setup of the proposed chaotic lidar is shown in Figure 1. The chaotic source consists of an 808 nm, 500 mW, single mode laser diode (LD), a aspheric collimating lens (AL), a coated beam splitter (BS, 30 : 70 R/T ratio), and a coated mirror (M). Feedback light with fixed feedback strength is reflected by M through BS. While the BS provides the feedback path, it also splits the chaotic light into the reference and probe light. The reference light is focused by a converging lens (L) and detected by a photo detector (PD). The probe light transmits through a beam expander to make the measurable range further. The reflected or backscattered light from the target is collected by a Maksutov-Cassegrain telescope and detected

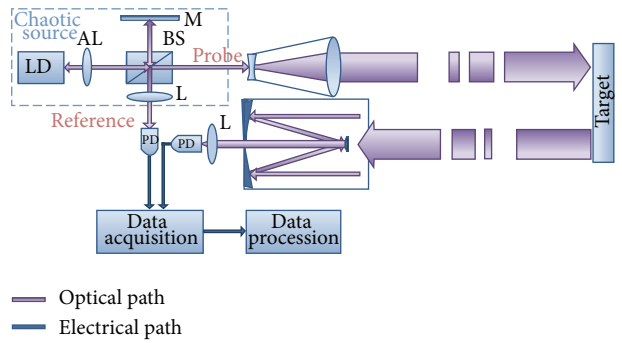

FIGURE 1: The schematic setup of the chaotic lidar. LD: laser diode; AL: aspheric collimating lens; BS: beam splitter; M: coated mirror; L: converging lens; PD: photo detector.

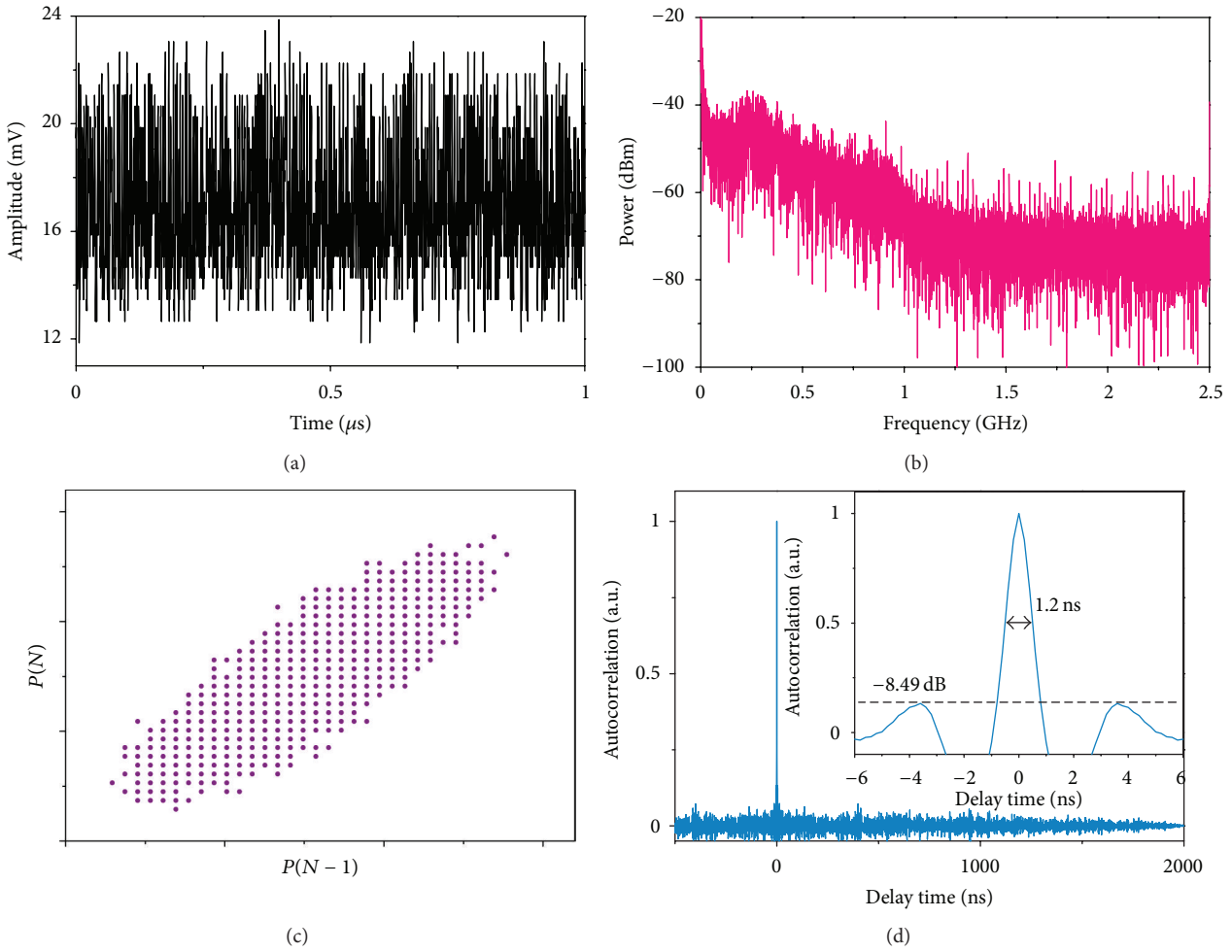

FIGURE 2: Chaotic states of the signal. (a) Time series. (b) Power spectrum. (c) Phase portrait. (d) Autocorrelation trace. The inset shows the FWHM and PSL of autocorrelation trace.

by another identical PD. The echo probe and reference light are converted into electrical signals and recorded by a data acquisition card. The cross-correlation of these two signals is calculated by the data processing system. The position of the target could be achieved from the main peak position in the correlation trace. The spatial resolution is determined by the full width at half maximum (FWHM) of the main peak of the correlation trace which is directly related to the bandwidth of the correlated signals.

The property of the chaotic signal from the chaotic source is shown in Figure 2. Figures 2(a)–2(d), respectively, show the time series, power spectrum, phase portrait, and autocorrelation trace. According to the time series, we can see that the chaotic signal vibrates in random form which makes it have a

Figure 3: Prototype of the chaotic lidar.

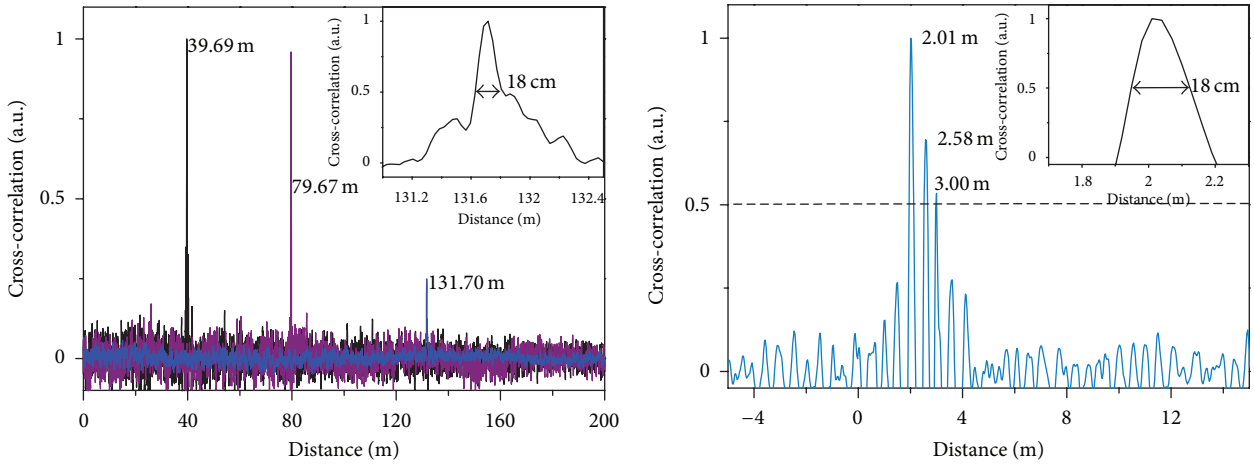

Figure 4: The ranging results of single target (a) and multiple targets (b).

perfect correlation trace as shown in Figure 2(d). The power spectrum is limited by the acquisition card with 500 MHz bandwidth. As illustrated in Figure 2(d), the FWHM is 1.2 ns corresponding to 18 cm resolution and the peak side-lobe level (PSL, the ratio of the maximum side-lobe to the peak of the correlation trace) is −8.49 dB. It should be pointed out that the FWHM is limited by our acquisition bandwidth.

According to the aforementioned experiment setup, we have developed a prototype of chaotic lidar. The front panel of chaotic lidar is shown in Figure 3. The port on the left launches the probe light and the other receives the reflected or backscattered light. Figure 4 displays the ranging results of single target and multiple targets. From Figure 4(a), we can see clearly that the peak in the cross-correlation trace which corresponds to the target at 36.69 m, 79.67 m, and 131.70 m, respectively. From the inside one, we can see that the FWHM of the cross-correlation at 131.70 m is 18 cm. Comparing with the FWHM in Figure 2(d), the spatial resolution is not influenced by the ranging distance. The main peak level of each correlation trace is decreased with increasing the distance between the instrument and, target. The maximum detective range is decided by the power of the probe light, the sensitivity of the receiver, and the dissipation of the transmission medium. And then we employ three targets at 2.01 m, 2.58 m, and 3.00 m reflecting part of the probe light to test the property of the multiple targets detection. As demonstrated in Figure 4(b), three targets are detected obviously and the spatial resolution is also 18 cm as shown in the insert one.

Furthermore, we analyze the dynamic range of the chaotic lidar according to the 3 dB criterion. That means when the maximum side-lobe value in correlation curve reaches to the half of the main peak level, the condition of the experiment will reflect the detection limit of the chaotic lidar. Restricted by our experimental condition, we place a variable neutral density filter behind the transmitting port to attenuate the output power and detect the single target. The value of the main peak level in the cross-correlation trace decreases as the attenuation increases. As shown in Figure 5, the side-lobe, which could be recognized as ghost peak, reaches half of the main peak level while attenuating −20 dB. Therefore, the dynamic range of the chaotic lidar is −20 dB, and it will be better when the output power is increased.

2.2. Antijamming Performance. In this part, we analyze the antijamming performance of the chaotic lidar experimentally and numerically. The chaotic signal, pulse signal, and sine modulated signal are chosen, respectively, as jamming sources. Each source influences the ranging result of the chaotic lidar to a certain extent. It should be pointed out that we have not taken any processing on the ranging results in this section.

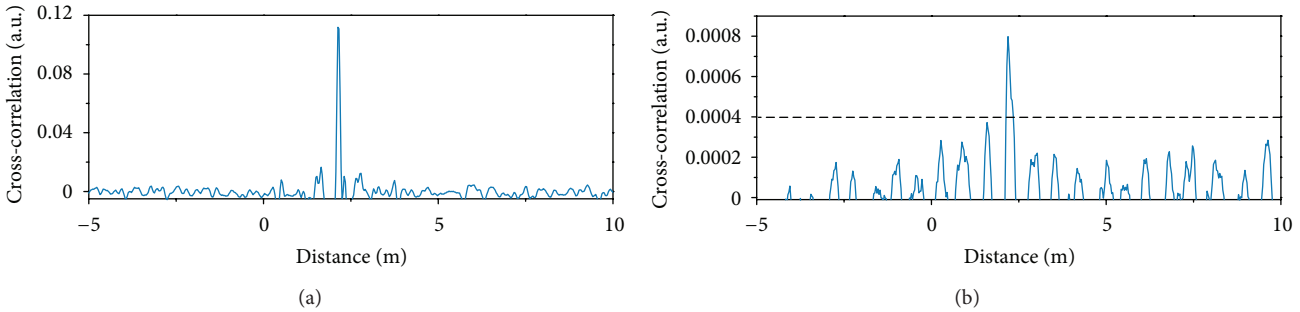

Figure 5: Cross-correlation with different attenuation of received light's strength. (a) 0 dB attenuation; (b) −20 dB attenuation.

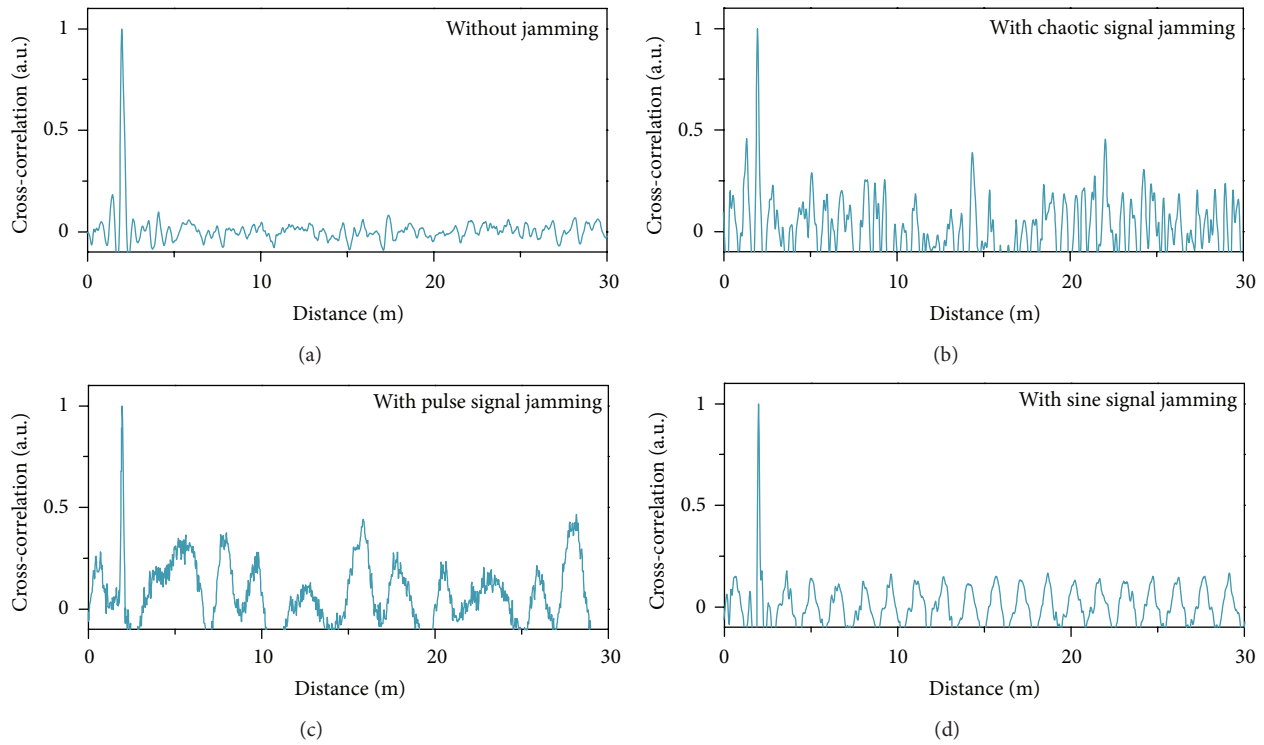

Figure 6: Ranging result without jamming (a), with chaotic signal jamming (b), with pulse signal jamming (c), and with sine signal jamming (d).

In experiments, we inject the jamming signal into the receiver of the chaotic lidar. Each ranging result is shown in Figure 6. One can observe that the noise level in cross-correlation curve is increased comparing with the result without jamming, but the main peak can still be identified easily. Moreover, the tolerance threshold of the chaotic lidar is analyzed in each interference pattern in the following paragraphs. Primarily, we define the SNR of chaotic lidar as the ratio of the correlation peak value to 3σ, where σ is the standard deviation of the side-lobe noise of correlation trace and 3σ implies that 99.7% noise is included. The signal-to-interference ratio (SIR) is defined as the ratio of the peak-to-peak value between probe signal and jamming signal.

Firstly, we examine the antijamming performance on chaotic signal interference, with fixing the intensity of probe signal and increasing another chaotic signal generated from the same configuration chaotic source. As shown in Figure 7(a), the SNR decreases with the increment of the chaotic jamming signal. If we use 3 dB criterion to identify the tolerance of the chaotic signal jamming in chaotic lidar, the threshold of SIR is −26.7 dB. Secondly, restricted by our experimental condition we simulate the situation of the jamming by pulse ranging system. Considering the normal parameters of the pulse ranging system with repetition rate of 10–100 kHz and pulse width of 5–30 ns, we choose the pulse signal with 6.3 ns width and 10 kHz repetition rate as the jamming signal. As the SIR of the pulse interference increases, the SNR of the correlation result decreases slowly. When the SNR reaches the 3 dB criterion in cross-correlation curve, the pulse level is higher than the probe signal 31.1 dB, as shown in Figure 7(b). Finally, we analyze the performance by jamming with sine modulated signal. According to the

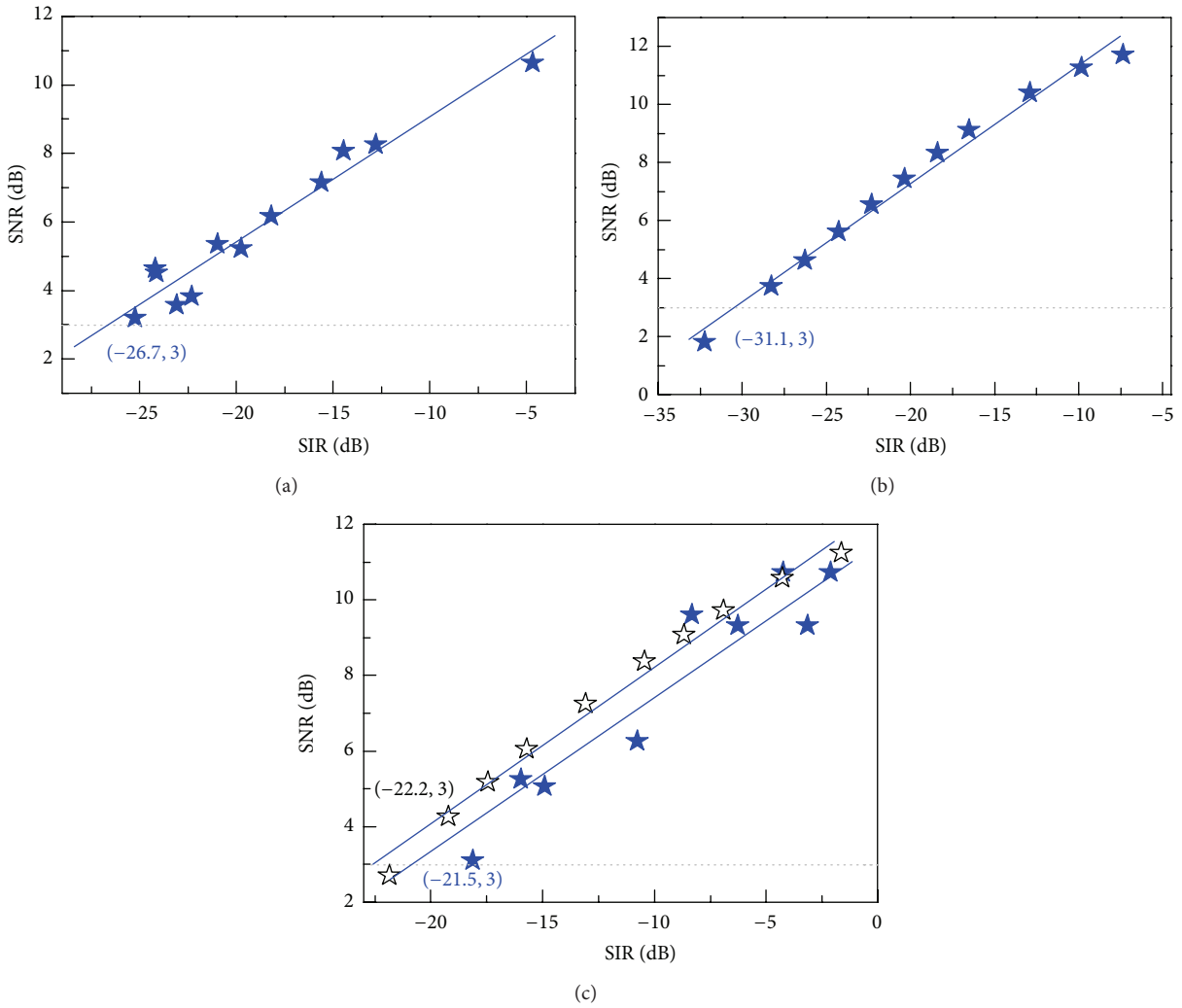

Figure 7: SNR as a function of SIR: jamming with chaotic signal (a), pulse signal (b), and sine signal (c).

usual modulation frequency of 10–1000 MHz, we utilize the sine modulated signal at 100 MHz to implement the following experiment and simulation. The results are shown in Figure 7(c), as filled star is experimental data and open star is numerical result. From these curves we can see that the ability of anti-jamming of sine modulated signal is −21.5 dB and −22.2 dB, respectively. Comparing with the interference situation of chaotic and pulse signal, the tolerance of the sine modulated signal interference is lower than 5 dB and 10 dB. However, the 21 dB anti-jamming performance of chaotic lidar is much higher than any of the other lidar systems. In addition, the spatial resolution is not affected by the jamming signal. Therefore, the chaotic lidar is greatly suitable for the extensive application where exists strong light interference.

In fact, excepting the strong interference from other ranging systems, the interference between the same type systems is the usual problem. Therefore, we simulate the situation of the ranging with same power and different number of jamming channels of chaotic signal interference. Here we use autocorrelation to demonstrate the ranging result instead of cross-correlation. Depending on the PSL, the contribution of the jamming signal can be explained. Each chaotic source is generated by the same model with different parameter, and the same power can be achieved by multiplying a factor in each generated result. Figure 8(a) shows the autocorrelation curves with (black) and without (gray) 30 channels jamming in 1000 ns correlation length. Obviously, the noise level does not increase much higher. Figure 8(b) depicts the result of the PSL as a function of the numbers of jamming channels. We can see that the curve rises slowly and turns into flat profile with the increment of the number of the jamming channels. This tendency reflects the noise-like character of chaotic signal further and also predicts that the chaotic lidar is hard to be interfered in the same ranging system.

2.3. Improvement of SNR. As aforementioned, the SNR is an important parameter for the ranging performance. Dreadful SNR will induce the target dropout or misjudgment. Sidelobe noise of correlation trace always increases due to the

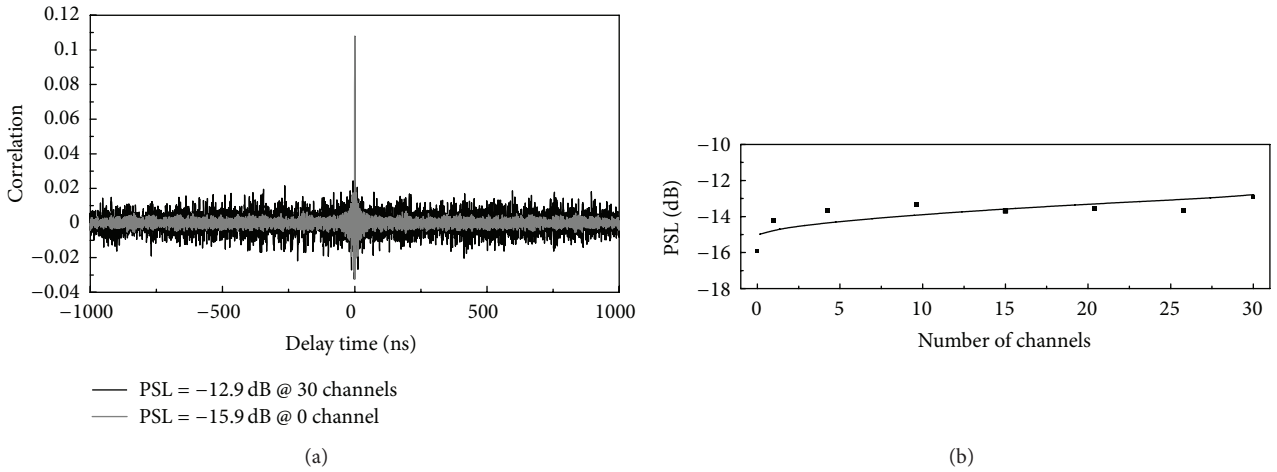

FIGURE 8: Ranging result with different channels in the same system's jamming. (a) Result with 30 channels of chaotic signal jamming; (b) PSL as a function of numbers of jamming channels.

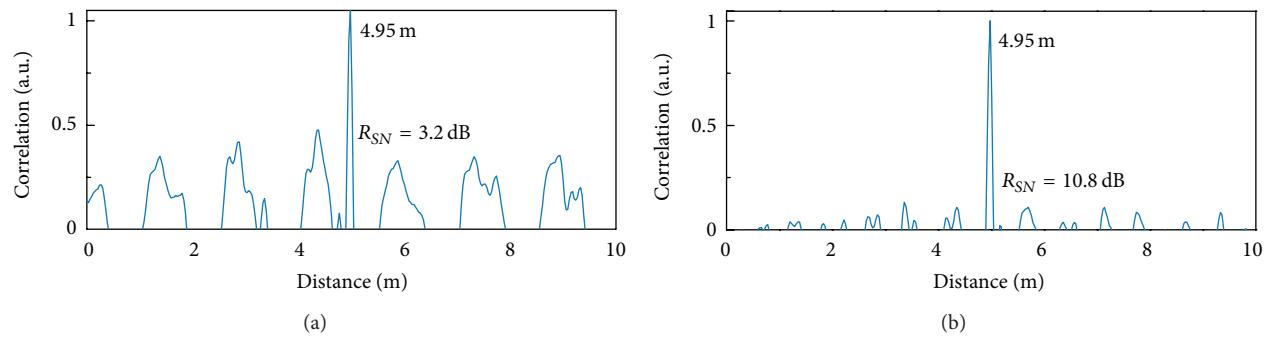

FIGURE 9: Ranging result with noised (a) and denoised (b) chaotic probe signal.

randomness of the chaotic signal itself and other transmission channel noises or interferences. Therefore, we must improve the SNR to achieve larger measureable range and weaker fault detection.

One way of the improvement is to adjust the parameter of the chaotic light generation system to alter the characteristic of the chaotic signal. This is the essential way to improve the SNR. And the other is to use the postprocessing method to optimize the received signals and the correlation result. It should be pointed out that we cannot modify the structure of the chaotic lidar prototype due to the integrated configuration. Here, we present two postprocessing methods to improve the SNR for the better ranging: the wavelet denoising method and the correlation average discrete-component elimination algorithm. We take examples with sine modulated signal jamming and chaotic signal jamming to analyze the improvement of each method.

The wavelet denoising method recovers the real chaotic lidar signal in strong period noise disturbance. The wavelet-based algorithm proposed by Donoho and Johnstone [11] attempts to recover a signal from noisy data. This algorithm can be completed in three steps: (1) wavelet transforms of the noisy signal; (2) thresholding the resulting wavelet coefficients; (3) inverse of wavelet transform to obtain the denoised signal.

The nonlinear shrinking of coefficients in the wavelet transform domain distinguishes this procedure from linear denoising methods. In the experiment, a continuous sine modulated laser signal (100 MHz, SIR = −17 dB) is chosen as the noise signal. The cross-correlation curve of the polluted chaotic probe signal is shown in Figure 9(a). We can observe that the noise seriously affects the identification of the target and the SNR is 3.2 dB. As shown in Figure 9(b), the denoised result improves the SNR to 10.8 dB. The SNR almost recovers to its level without noise disturbance.

The correlation average discrete-component elimination algorithm can significantly suppress the side-lobe noise of the correlation trace. It requires one to calculate the auto-correlation of the reference and the cross-correlation of the reference and echoed probe signal several times just the same as the average times. Autocorrelation and cross-correlation results are respectively averaged and normalized to prepare the next processing. And then it should align the main peak of the auto- and cross-correlation trace. After subtracting the autocorrelation sequence from cross-correlation sequence excluding the point of the main peak, the inherent side-lobe noise is almost eliminated in the correlation of the chaotic signal. Figure 10(a) shows the ranging result with interference noise which used another 20 dB strong chaotic signal embedding into probe. The improvement of the ranging result's SNR

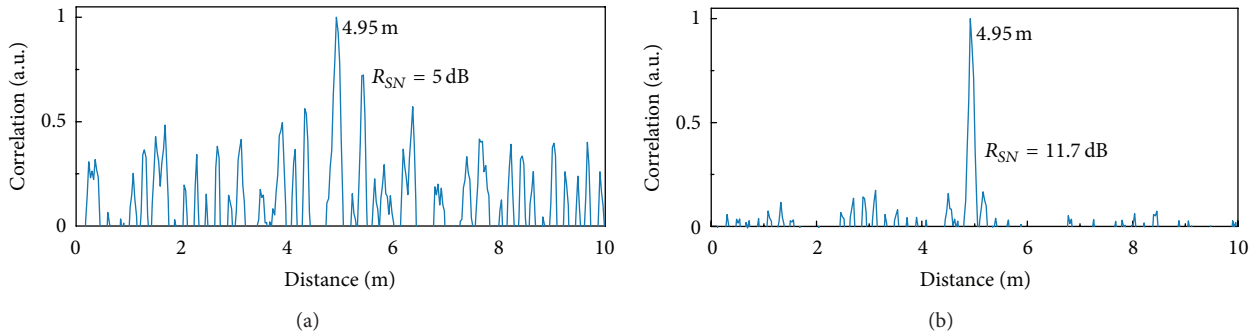

FIGURE 10: Ranging result without (a) and with (b) the use of correlation average discrete-component elimination algorithm.

by the correlation average discrete-component elimination algorithm is shown in Figure 10(b). Obviously, the SNR is improved from 5 dB to 11.7 dB.

3. Conclusions

In summary, we have proposed a chaotic lidar for free space target ranging and developed a prototype. It can range at least 130 m with the constant spatial resolution of 18 cm and the sensitivity is −20 dB. Experiment results demonstrate that both single and multiple targets can be detected. The anti-jamming performance is studied in three different interference systems. The wavelet denoising method is proposed to eliminate low frequency noise disturbance and the correlation average discrete-component elimination algorithm is employed to suppress the side-lobe noise in correlation result. We believe that the chaotic lidar is a promising candidate for long distance ranging with high spatial resolution in low loss transmission medium, and the high accuracy imaging can be achieved with the help of rotating mirror.

Acknowledgment

This work was supported by the National Natural Science Foundation of China (NSFC) (Grant nos. 60908014, 60927007, 61108027, and 61205142), the Key Science and Technology Program (20100321055-02) of Shanxi Province, Shanxi Scholarship Council of China, and the Program for the Outstanding Innovative Teams of Higher Learning Institutions of Shanxi, China (OIT).

References

[1] H. Tang, R. Dubayah, A. Swatantran et al., "Retrieval of vertical LAI profiles over tropical rain forests using waveform lidar at La Selva, Costa Rica," *Remote Sensing of Environment*, vol. 124, pp. 242–250, 2012.

[2] M. U. Piracha, D. Nguyen, D. Mandridis et al., "Range resolved lidar for long distance ranging with sub-millimeter resolution," *Optics Express*, vol. 18, no. 7, pp. 7184–7189, 2010.

[3] M. Jaboyedoff, T. Oppikofer, A. Abellán et al., "Use of LIDAR in landslide investigations: a review," *Natural Hazards*, vol. 61, no. 1, pp. 15–28, 2012.

[4] N. Takeuchi, N. Sugimoto, H. Baba, and K. Sakurai, "Random modulation cw lidar," *Applied Optics*, vol. 22, no. 9, pp. 1382–1386, 1983.

[5] K. Myneni, T. A. Barr, B. R. Reed, S. D. Pethel, and N. J. Corron, "High-precision ranging using a chaotic laser pulse train," *Applied Physics Letters*, vol. 78, no. 11, pp. 1496–1498, 2001.

[6] F. Y. Lin and J. M. Liu, "Chaotic lidar," *IEEE Journal on Selected Topics in Quantum Electronics*, vol. 10, no. 5, pp. 991–997, 2004.

[7] T. Zhao, B. J. Wang, A. B. Wang, and Y. C. Wang, "A laser ranging system using chaotic light," *Journal of Measurement Science and Instrumentation*, vol. 2, pp. 398–401, 2011.

[8] T. Zhao, A. B. Wang, and Y. C. Wang, "Two laser ranging instruments using chaotic light," in *Proceedings of the International Conference on Optical Instruments and Technology (OIT '11)*, vol. 82010C, International Society for Optics and Photonics, 2011.

[9] B. J. Wang, J. J. Qian, T. Zhao, Y. C. Wang, and H. K. Wang, "Anti-jamming performance of chaotic lidar," *Chinese Journal of Lasers*, vol. 38, no. 5, Article ID 0514002, 2011.

[10] B. J. Wang, T. Zhao, and H. K. Wang, "Improvement of signal-to-noise ratio in chaotic laser radar based on algorithm implementation," *Chinese Optics Letters*, vol. 10, Article ID 052801, 2012.

[11] D. L. Donoho and J. M. Johnstone, "Ideal spatial adaptation by wavelet shrinkage," *Biometrika*, vol. 81, no. 3, pp. 425–455, 1994.